Inorganic Chemistry

Article

pubs.acs.org/IC

Dimensional Reduction From 2D Layer to 1D Band for Germanophosphates Induced by the "Tailor Effect" of Fluoride

Chun-Zuo Huang,[†] Biao Liu,[†] Lei Wen,[†] Rong-Chuan Zhuang,[‡] Jing-Tai Zhao,[#] Yuanming Pan,[§] Jin-Xiao Mi,[†] and Ya-Xi Huang*[,†]

[†]Fujian Provincial Key Laboratory of Advanced Materials, Department of Materials Science and Engineering, College of Materials, Xiamen University, Xiamen 361005, China

[‡]Xiamen Zijin Mining and Metallurgy Technology Co Ltd., Xiamen 361101, China

[#]School of Materials Science and Engineering, Shanghai University, Shangda Road No. 99, Shanghai 200072, China

[§]Department of Geological Sciences, University of Saskatchewan, 114 Science Place, Saskatoon, SK S7N5E2, Canada

Supporting Information

ABSTRACT: The "tailor effect" of fluoride, exclusively as a terminal rather than a bridge, was applied successfully to design low-dimensional structures in the system of transition metal germanophosphates for the first time. Two series of new compounds with low-dimensional structures are reported herein. $K[M^{II}Ge(OH)_2(H_{0.5}PO_4)_2]$ (M = Fe, Co) possess flat layered structures built from single chains of edge-sharing $M^{II}O_6$ and GeO_6 octahedra interconnected by HPO_4 tetrahedra. Their fluorinated derivatives, $K_4[M^{II}Ge_2F_2(OH)_2(PO_4)_2(HPO_4)_2]\cdot 2H_2O$ (M = Fe, Co), exhibit band structures of two four-membered ring germanium phosphate single chains sandwiched by $M^{II}O_6$ octahedra via corner-sharing. Both of these structures contain anionic chains of the condensation of four-membered rings built from alternating $GeO_4\Phi_2$ (Φ = F, OH) octahedra and PO_4 tetrahedra via sharing common $GeO_4\Phi_2$ (Φ = F, OH) octahedra, the topology of which is the same as that of the mineral kröhnkite $[Na_2Cu(SO_4)_2\cdot 2H_2O]$. Note that the switch from the two-dimensional layered structure to the one-dimensional band structure was performed simply by the addition of a small amount of $KF\cdot 2H_2O$ to the reaction mixture. This structural alteration arises from the incorporation of one terminal F atom to the coordination sphere of Ge, which breaks the linkage between the transition metal and germanium octahedra in the layer to form the band structure.

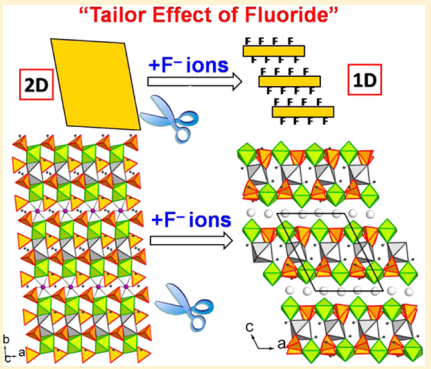

1. INTRODUCTION

Materials with low-dimensional structures have been widely applied in the field of high-performance coating for their low dispersive energy and power source arising from their large surface area and high ion mobility.[1] Also, low-dimensional structures have been proposed to be important components to design high-dimensional structures.[2−4] For example, Ozin and co-workers postulated that three-dimensional (3D) aluminum phosphates might form from low-dimensional motifs, namely, metastable chain and layer phases.[3] Indeed, synthesis of new materials with low-dimensional structures is becoming an active research area from the viewpoint of both fundamental study and industrial applications.[5,6] Currently, two common strategies have been developed and employed to synthesize compounds with low-dimensional structures. The first one is the space inhibition effect by adding large organic molecules, such as amines, into the synthetic media, which can be found in organically templated aluminophosphates.[7] The other method is to introduce fluoride into the inorganic framework structures because F^- ions, compared with the bridging manner of O^{2-} ions, prefer to reside at terminal positions, which in turn inhibit further connections, for example, fluorinated germanates[8] and metal fluorophosphates,[9] to yield low-dimensional structures. However, F^- ions can also act as bridging ions in the crystal structure except for as-discussed above at terminal positions. To rationally design synthesis of F^- ions exclusively at terminal positions is rather tricky. In this article, the fluoride method was applied successfully to design new compounds with low-dimensional structures in the system of germanophosphates (GePOs) for the first time.

GePOs is a young system in the metal phosphate family. Recently, metal phosphates have drawn much attention not only for their rich structural chemistries[10] but also for their widespread applications in catalysts[11] and lithium batteries.[12,13] However, information about the crystal structures and physical properties of GePOs is very limited, and this is the main reason hindering its further application. Therefore, it is timely to explore new GePOs with novel structure types and properties.

To date, most of the known GePOs compounds, including nonmetal GePOs,[14] alkali and alkaline earth metal GePOs,[15−19] and transition metal GePOs,[20−25] are characterized by 3D

Received: April 30, 2015
Published: June 26, 2015

DOI: 10.1021/acs.inorgchem.5b00973
Inorg. Chem. 2015, 54, 6978−6985

Scheme 1. Typical Synthetic Procedures of KFeGePO-2 (a) and KFeGePOF (b)

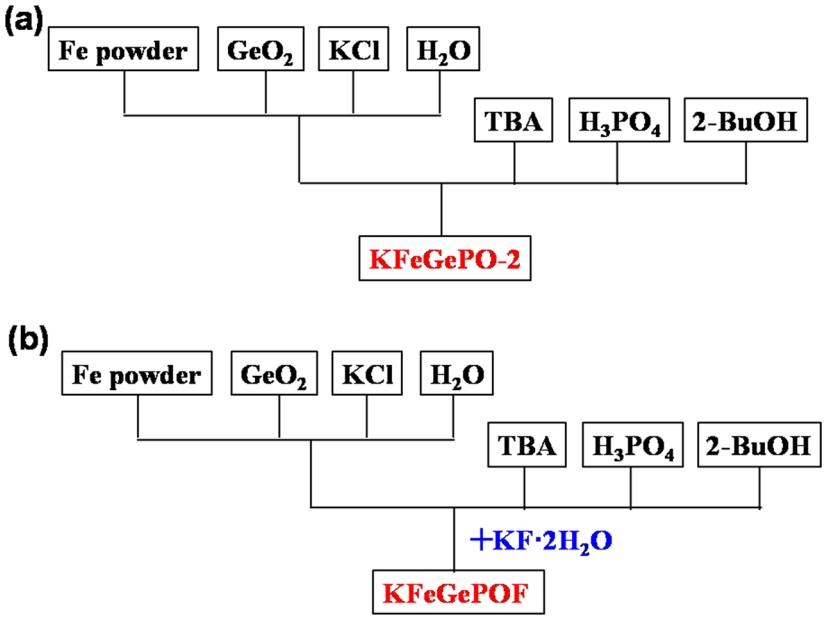

structures. For the alkali and alkaline earth metal GePOs, its high dimensionality may be attributable to the high-temperature solid-state methods applied to synthesize them, for example, the alkali metal GePOs with the NASICON structure[15−18] and the KTP structure.[26] Additionally, because of the good affinity between transition metals and phosphates, transition metal octahedra are often connected with phosphates in transition metal GePOs. Consequently, all transition metal GePOs known until now show exclusively 3D framework structures. However, three GePOs compounds with low-dimensional structures in the GePO system without any transition metal have been reported. Two of them (α-$Ge(HPO_4)_2{\cdot}H_2O$[27,28] and $CsGe(PO_4)_4$[18]) possess layered structures. The third one, $(NH_4)_2[Ge(NH_3)_2(PO_4)_2]{\cdot}0.38H_2O$, of the one-dimensional (1D) chain structures, was synthesized from the low-temperature ionothermal method.[29] As a continuous work of our systematic investigation on transition metal GePOs,[24,25] a series of new two-dimensional (2D) layered compounds with the general formula $K[M^{II}Ge(OH)_2(H_{0.5}PO_4)_2]$ (M = Fe, Co; designated as KFeGePO-2 and KCoGePO-2, respectively) and another series of their fluorinated derivatives with 1D band structures, $K_4[M^{II}Ge_2F_2(OH)_2(PO_4)_2(HPO_4)_2]{\cdot}2H_2O$ (M = Fe, Co; designated as KFeGePOF and KCoGePOF, respectively), were synthesized by using a low-temperature solvo-hydrothermal method in the absence and presence of $KF{\cdot}2H_2O$, respectively. The addition of $KF{\cdot}2H_2O$ to the reaction mixture not only changes the coordination sphere of germanium but also leads to the structural change from the 2D layer to the 1D band, induced by the "tailor effect" of F^- ions.

2. EXPERIMENTAL SECTION

2.1. Synthesis. An unconventional hydrothermal method was applied to synthesize the title compounds. Specifically, the reaction medium used is not pure water but a mixture of organic solvents (2-butanol (2-BuOH)) and water, in conjunction with tripropylamine (TPA)/tributylamine (TBA) as structure-directing agents. A typical synthetic procedure is presented in Scheme 1. Take KFeGePO-2 as an example. GeO_2 (0.07 g, 0.7 mmol), KCl (0.149 g, 2.0 mmol), and Fe powder (0.014 g, 0.25 mmol) were first added to 2 mL of H_2O (14.6 mmol) under stirring. Then TBA (3 mL, 21.6 mmol) and 2-BuOH (2 mL, 21 mmol) were added to the above solution dropwise. Finally, H_3PO_4 (85%, 0.75 mL, 11 mmol) was added under constant stirring. The final mixture with an initial pH value of ∼5 was transferred into a Teflon-lined stainless-steel autoclave (15 mL in volume, filling degree 50%) and heated at 190 °C for 5 d under static conditions. After that the autoclaves were removed from the oven and cooled in air. The solid products, which were filtered, washed with deionized water, and dried in air, consist of colorless blocky crystals (see Figure 1a) in high yield (∼70%, based on Ge). The crystallinity and phase purity of the resulting products were examined by applying the powder X-ray diffraction (PXRD) method. The observed PXRD pattern agrees well with the structure determined from single-crystal X-ray diffraction data (see Figure 2a). For KCoGePO-2, a similar synthetic procedure was applied, but $CoCl_2{\cdot}6H_2O$, KH_2PO_4, and TPA take the place of Fe powder, KCl, and TBA, respectively. The pure phase was prepared with the reactants molar ratio of $GeO_2/CoCl_2{\cdot}6H_2O/KH_2PO_4/H_3PO_4$ = 1:0.5:1:14.4. The existence of the elements K, Fe/Co, Ge, and P in KMGePO-2 was confirmed by energy-dispersive X-ray spectroscopy (see Figure S1 in the Supporting Information).

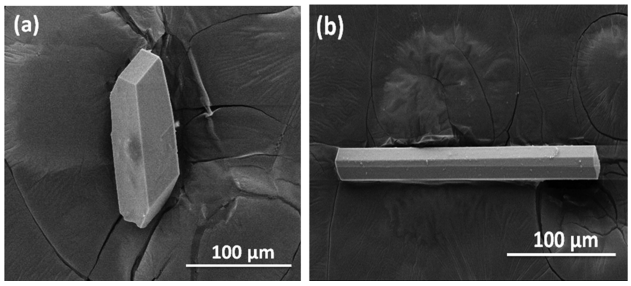

Figure 1. SEM images of the single crystals of KFeGePO-2 (a) and KFeGePOF (b).

For the synthesis of fluorinated compounds, experiments with the same conditions as those for KFeGePO-2, including the reactant molar ratio, mixing sequence, reaction temperature, reaction time, and so on, but with the addition of 0.094 g of $KF{\cdot}2H_2O$ (1 mmol; see Scheme 1b), resulted in the formation of colorless crystals with rodlike shape (Figure 1b). The PXRD pattern of these rodlike crystals is completely different from that of KFeGePO-2. These crystals are subsequently identified as a new phase KFeGePOF (see Figure 2b). An energy-

DOI: 10.1021/acs.inorgchem.5b00973
Inorg. Chem. 2015, 54, 6978−6985

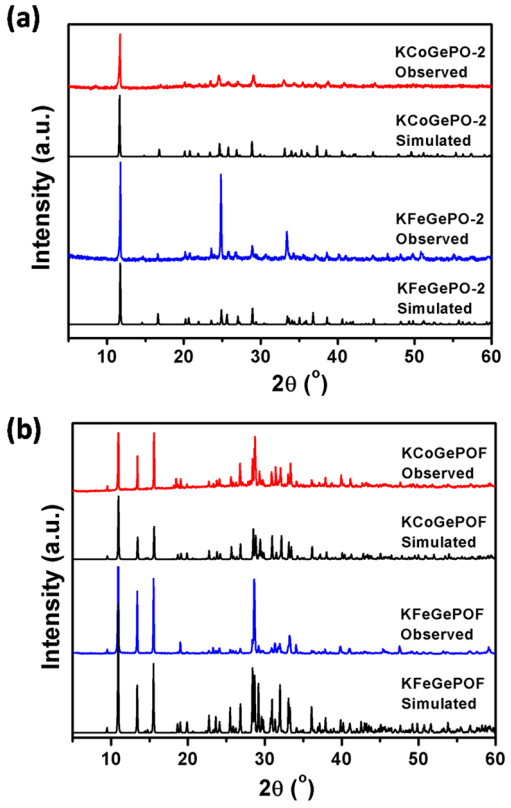

Figure 2. PXRD patterns of K*M*GePO-2 (*M* = Fe, Co) (a) and K*M*GePOF (*M* = Fe, Co) (b) show their isostructural properties and good agreement between observed and simulated patterns. Cu Kα radiation.

dispersive X-ray spectroscopy analysis confirms the existence of the additional element F in this compound.

Systematic synthesis experiments showed that both nonfluorinated compounds can be obtained in the composition range of (0.7−1) GeO_2: (0.5/1) $CoCl_2{\cdot}6H_2O$/Fe: (3.6/21.6) TPA/TBA: (111) H_2O: (3.67−11) H_3PO_4: (21) 2-BuOH, while the fluorinated derivatives require only the addition of (1−2) $KF{\cdot}2H_2O$. The reaction temperatures can be in the range of 190−240 °C. Note that higher temperatures, that is, at 240 °C, did not lead to any 3D structure compound. Also, longer reaction times (up to 7 d) did not form any higher-dimensional compound. However, for the nonfluorinated compounds, excessive H_3PO_4, for example, more than 11 mmol, resulted in pure KFe(Co)GePO-1[25] with a 3D framework structure reported by our group recently.

To understand the effects of fluoride on the formation of KFeGePOF, we performed a series of experiments by changing the amount of $KF{\cdot}2H_2O$. The addition of 1−2 mmol $KF{\cdot}2H_2O$ led to KFeGePOF. However, 3−5 mmol $KF{\cdot}2H_2O$ resulted in a mixture of $K_3HGe_7O16{\cdot}4H_2O$, FeF_3, and KH_2PO_4. When the amount of $KF{\cdot}2H_2O$ exceeded 7 mmol, only KH_2PO_4 formed as the solid product.

The effect of pH values on the formation of KFeGePOF was also explored by varying the amount of H_3PO_4 or by adding KOH. When the pH value was lower than 4.5 by adding 2 mL of H_3PO_4, it did not form the expected KFeGePOF compound but an unidentified phase. When the pH value is close to 9 by adding KOH up to 12 mmol, KFeGePOF remains as the unique solid product. These results show that the optimal condition for the formation of KFeGePOF is near neutral pH.

2.2. Methods. The PXRD patterns were recorded on a Bruker D8 Advance X-ray powder diffractometer (Cu Kα radiation, Ni filter). The morphologies and some element contents of the synthesized compounds were observed using a field-emission scanning electron microscope (FE-SEM, LEO-1530) equipped with energy-dispersive X-ray spectrometry. Fourier transform-infrared (FT-IR) spectra were recorded on a Thermo Scientific Nicolet iS10 FT-IR Spectrometer

Table 1. Details of the Data Collections and Selected Refinement Results for KFeGePO-2, KCoGePO-2, KFeGePOF, and KCoGePOF

compound	KFeGePO-2	KCoGePO-2	KFeGePOF	KCoGePOF
formula	$K[Fe^{II}Ge(OH)_2(H_{0.5}PO_4)_2]$	$K[CoGe(OH)_2(H_{0.5}PO_4)_2]$	$K_4[Fe^{II}Ge_2F_2(OH)_2(PO_4)_2(HPO_4)_2]{\cdot}2H_2O$	$K_4[CoGe_2F_2(OH)_2(PO_4)_2(HPO_4)_2]{\cdot}2H_2O$
space group	triclinic, $P\bar{1}$	triclinic, $P\bar{1}$	monoclinic, $P2_1/c$	monoclinic, $P2_1/c$
a(Å)	4.4538(9)	4.4540(1)	9.968(4)	9.946(4)
b(Å)	6.2232(13)	6.1119(14)	16.193(6)	16.132(7)
c(Å)	7.8158(17)	7.783 83(18)	12.750(4)	12.653(4)
α(deg)	102.384(3)	102.020(3)	90	90
β(deg)	97.350(3)	97.210(3)	116.49(2)	116.19(3)
γ(deg)	92.227(3)	91.750(3)	90	90
V(Å^3)/Z	209.36(8)/1	206.70(8)/1	1841.9(12)/4	1821.6(12)/4
ρ_{calcd} (g cm^{-3})	3.113	3.178	3.056	3.101
μ(mm^{-1})	6.241	6.573	5.396	5.57
crystal size (mm^3)	0.11 × 0.07 × 0.03	0.12 × 0.08 × 0.04	0.1 × 0.05 × 0.03	0.1 × 0.08 × 0.02
radiation (Å)	Mo Kα, 0.710 73	Mo Kα, 0.710 73	Mo Kα, 0.710 73	Mo Kα, 0.710 73
temperature (K)	173(2)	173(2)	173(2)	173(2)
R_{int}/R_σ	0.0126/0.0205	0.0155/0.0233	0.0000/0.0717	0.0412/0.0578
unique reflections (all/$I > 2\sigma(I)$)	935/908	921/898	4249/3294	4373/3492
no. of refined parameters	83	79	325	325
R_1 ($I > 2\sigma(I)$)	0.0298	0.025	0.051	0.0419
wR_2 (all data)	0.0706	0.064	0.106	0.1025
GOF (for F^2)	1.121	1.076	1.028	1.036
$\Delta\rho_{max}$(e Å^{-3}) negative/positive	−0.458/0.656	−0.615/0.569	−0.857/1.224	−0.788/1.328

DOI: 10.1021/acs.inorgchem.5b00973
Inorg. Chem. 2015, 54, 6978−6985

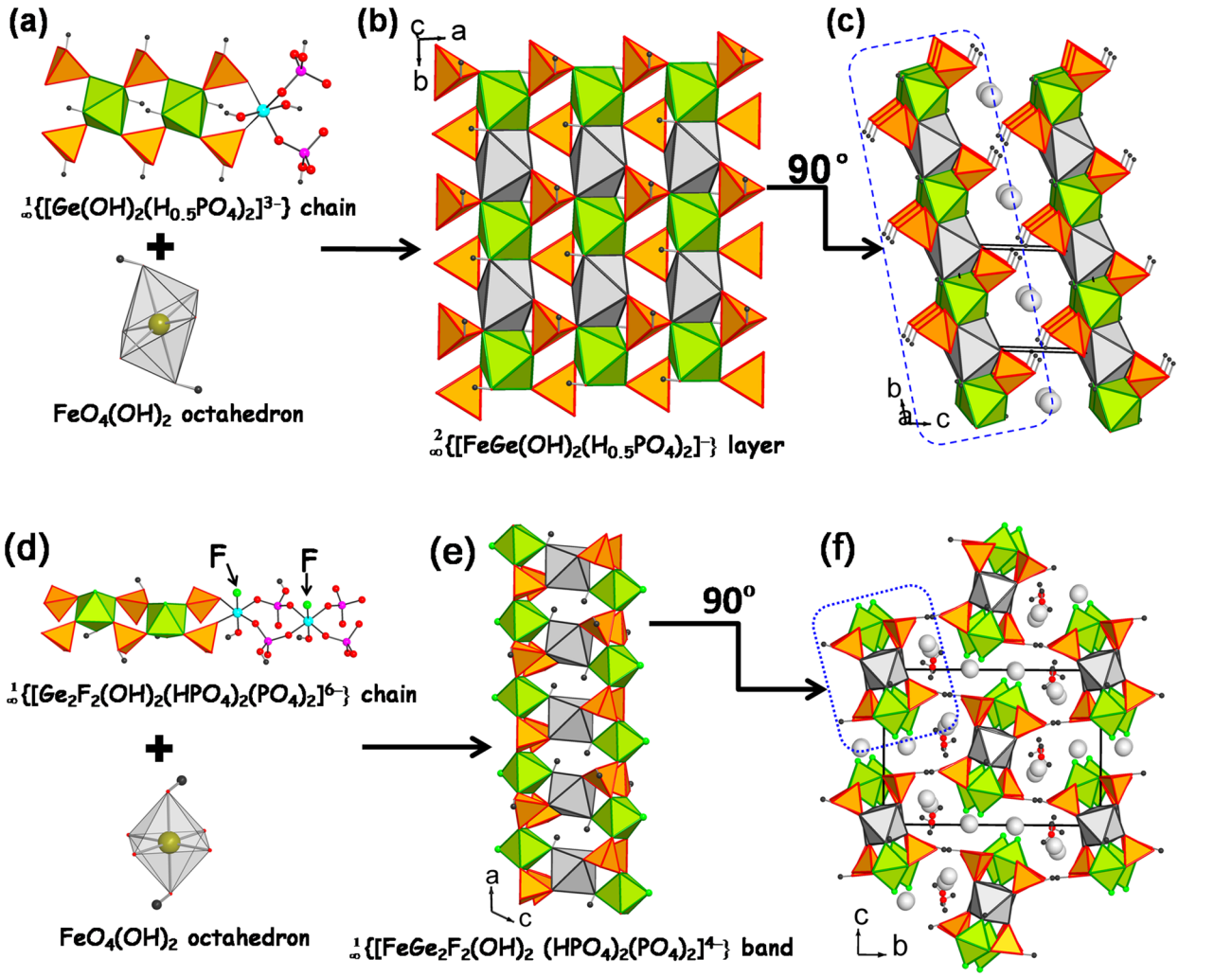

Figure 3. Crystal structure conformation of KFeGePO-2 (a–c) and KFeGePOF (d–f). $GeO_4(OH)_2$/$GeO_4(OH)F$ octahedra: green, PO_4 tetrahedra: orange, K atoms: light gray spheres, Fe atoms: brown spheres, Ge atoms: turquoise spheres, P atoms: purple spheres, F atoms: green spheres, O atoms: red spheres, H atoms: small dark gray spheres.

equipped with a smart endurance single-bounce diamond attenuated total reflectance cell in the range from 400 to 4000 cm^{-1}. Thermogravimetric analyses (TGA) were investigated on STD Q600 (TA Instruments) with a heating rate of 10 K·min^{-1} from room temperature to 800 °C in a nitrogen gas flow of 100 mL·min^{-1}. The magnetic properties were investigated on a Quantum Design MPMS-7T superconducting quantum interference device (SQUID) magnetometer in the temperature range of 2–300 K.

2.3. Crystal Structure Determination. Suitable single crystals of the reported compounds were selected under a polarized microscope prior to single-crystal X-ray diffraction measurements. All data for four new compounds were collected on a Bruker diffractometer with graphite monochromated Mo Kα radiation (λ = 0.710 73 Å, 50 kV/40 mA, scan type ω) at 173(2) K. The crystal structures were solved (KFeGePO-2 and KCoGePO-2 crystallized in space group $P\bar{1}$, KFeGePOF, and KCoGePOF in space group $P2_1/c$) by direct methods and refined by full-matrix least-squares methods using the SHELX programs.[30] M^{II}, Ge, P, and some of their coordinated atoms like F and O were determined by direct methods. The crystal waters as well as the K sites were located from the difference Fourier maps. It is important to note that, in KMGePO-2, the H2 atoms bonded to the phosphate groups were found to locate at the center between the O2 atoms of the phosphate groups in neighboring layers with the O2–H2 distance of 1.2 Å, which is too far for general O–H distance. A similar hydrogen location had been observed in $Li_2Fe[(PO_4)(HPO_4)]$,[31] which also has an anomalous O–H distance of 1.2–1.3 Å. The H atom in $Li_2Fe[(PO_4)(HPO_4)]$ was subsequently shown to be positioned off the symmetry center by high-quality refinements using very good diffraction data. Using a similar approach, the H2 position in KMGePO-2 was also geometrically constrained to the O–H distance of 0.82 Å with half occupancy. The half occupancy of H2 is supported by bond valence sum calculations,[32] which gave 1.31 valence unit for the O2 atom in KFeGePO-2. This value indicates that only half occupancy of H contributes to the valence of O2. In addition, bond valence sum calculations show that the Fe atoms in both compounds have the +2 oxidation state (see Supporting Information). Relevant crystallographic details of the title compounds are given in Table 1. Selected bond lengths and angles, bond valence sums, and additional crystallographic information are given in Supporting Information.

3. RESULTS AND DISCUSSION

3.1. Crystal Structure Description. *KFeGePO-2.* X-ray structure analyses reveal that KFeGePO-2 and KCoGePO-2 are isostructural and crystallize in the space group $P\bar{1}$ with a 2D layered structure, whereas KMGePOF (M = Fe, Co), also isostructural, crystallizes in the space group $P2_1/c$ with a 1D band structure. Therefore, KFeGePO-2 and KFeGePOF are chosen below as the examples to discuss the structures and properties of these two series of new GePOs compounds.

The layered structure of KFeGePO-2 (Figure 2) is made of four-ring GePO single chains, $^1_\infty\{[Ge(OH)_2(H_{0.5}PO_4)_2]^{3-}\}$,

DOI: 10.1021/acs.inorgchem.5b00973
Inorg. Chem. 2015, 54, 6978–6985

interconnected by $FeO_4(OH)_2$ octahedra. The four-ring GePO single chain (Figure 3a) is made of a "composite building unit" (CBU) consisting of one $GeO_4(OH)_2$ octahedron and two HPO_4 tetrahedra. The condensation of CBUs forms an infinite $^1_\infty\{[Ge(OH)_2(H_{0.5}PO_4)_2]^{3-}\}$ single chain consisting of four-membered rings (Ge−P−Ge−P) along the *c*-axis. Hence, a $GeO_4(OH)_2$ octahedron shares its four equatorial O-corners each with a HPO_4 tetrahedron, while each phosphate tetrahedron shares two corners with neighboring $GeO_4(OH)_2$ octahedra. The iron octahedra share the common O−O edges with $GeO_4(OH)_2$ octahedra and the O-corners with HPO_4 tetrahedra, resulting in iron GePO layers (FeGePO layer) parallel to the *ab*-plane. The FeGePO layers are stacked along the *c*-axis with the hydrogen atoms of HPO_4 tetrahedra protruding to the interlayer space. Consequently, the interlayer space is reduced by the protruding H atoms to form a pseudochannel running along the *a*-axis, which is filled by K^+ ions. Here, K^+ ions not only balance the negative charge of the layers but also connect to 10 O atoms of the FeGePO layers to form a 3D structure. In addition, the FeGePO layers are also interconnected by strong hydrogen bonds (O2−H2···O2) between neighboring layers.

KFeGePOF. The crystal structure of KFeGePOF (see Figure 3) is made of iron fluoroGePO single bands (Figure 3e) separated by K^+ ions and H_2O molecules. The single band, running along the *a*-axis, is built from two four-ring fluorogermanophosphate single chains (GePOF chain) sandwiched by $FeO_4(OH)_2$ octahedra. The $FeO_4(OH)_2$ octahedron, lying at the center of the two GePOF chains, shares its trans-OH apexes with $GeO_4F(OH)$ octahedra and its four equatorial O corners with two PO_4 tetrahedra and two HPO_4 tetrahedra (see Figures 3e and 4b). The GePOF chain is also built from Ge−P−Ge−P four-membered rings the same as that in KFeGePO-2. However, in the coordination sphere of Ge, one of the two bridging hydroxyl groups is replaced by a terminal F^- ion. The FeGePOF bands stack parallel along the *c*-axis and crosswise arrange along the *b*-axis. The neighboring FeGePOF bands are linked by K^+ ions, which are coordinated by nine or ten O/F atoms of the FeGePOF layers and water molecules. Here K^+ ions also balance the negative charge of the single bands.

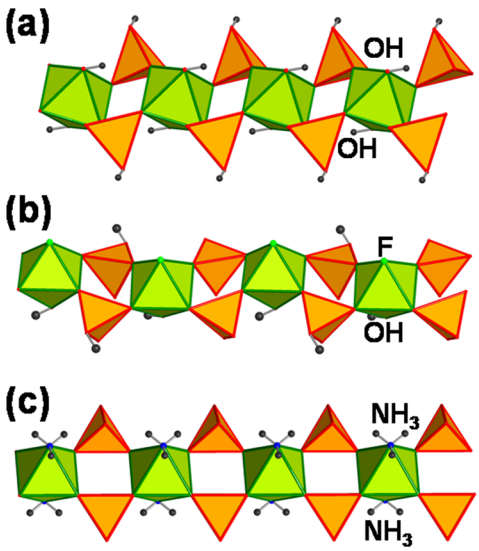

Figure 4. Kröhnkite-type single chains in GePOs are shown for comparison: (a) KFeGePO-2; (b) KFeGePOF; (c) $(NH_4)_2[Ge(NH_3)_2(PO_4)_2]\cdot 0.38H_2O$.[29] $GeO_4(OH/F/NH_3)_2$ octahedra: green, PO_4 tetrahedra: orange, H atoms: dark gray spheres.

It is worthwhile to note that the GePO single chain consisting of four-membered rings (Ge−P−Ge−P) is one of the simplest and the most common single chain in metal phosphates. Many examples of such chains have been reported in gallium,[33] zirconium,[34] and vanadium phosphates.[35] This type of single chain is also similar to that observed in the mineral copper sulfate kröhnkite $(Na_2Cu(SO_4)_2\cdot 2H_2O)$.[36] Furthermore, it is interesting to find that the two apical species of the Ge octahedra in GePOs are variable, for example, O, OH, F, and even NH_3. In the title compounds, only OH groups are found in KFeGePO-2 (see Figure 4a), but both an OH group and a F^- ion occur in KFeGePOF (Figure 4b). A substitution of NH_3 for the OH groups occurs in the previously reported GePO, $(NH_4)_2[Ge(NH_3)_2(PO_4)_2]\cdot 0.38H_2O$,[29] in which the NH_3 groups are the in situ decomposition products of urea. In other words, the rich coordination species of Ge also lead to rich crystal structures.

3.2. Structural Transformation. With a closer inspection of the crystal structures of KFeGePO-2 and KFeGePOF, obviously these two types of structures are closely related. Specifically, the band structure of KFeGePOF can be derived from the layered structure of KFeGePO-2, as illustrated in Figure 5. The part illustrated by polyhedra in KFeGePO-2 (Figure 5b) is strikingly similar to the band structure of KFeGePOF (Figure 5c). The only difference lies in the interconnection manner between $FeO_4(OH)_2$ and $GeO_4(OH)_2/GeO_4F(OH)$ octahedra. Edge sharing is found in KFeGePO-2, whereas corner sharing is present in KFeGePOF. This difference is caused by the replacement of one of the two hydroxyl groups in the Ge coordination sphere of KFeGePO-2 by a fluorine in KFeGePOF. Because fluorine prefers to be a terminal rather than bridging species, it not only removes half of the iron octahedra in the layered structure but also breaks the edge sharing between Fe- and Ge-octahedra in the band structure, where the F atom is oriented toward the interband space in the *ac*-plane. Additionally, to balance the charge, K atoms in KFeGePOF take half of the iron positions in KFeGePO-2, which are illustrated by balls and sticks in Figure 5b. Therefore, a structural transformation from the 2D layer to the 1D band via the tailor effect of F^- ions was observed. This transformation can also be represented by the following formula relationship:

$$2 \times K[FeGe(OH)_2(H_{0.5}PO_4)_2] \quad (\text{“}K_2[Fe_2Ge_2(OH)_4(H_{0.5}PO_4)_4]\text{”})$$
$$\xrightarrow[\text{isoelectronic}]{+2K^+,-Fe^{2+},+2F^-,+2H^+} K_4[FeGe_2F_2(OH)_2(PO_4)_2(HPO_4)_2]\cdot 2H_2O$$

The structural alternation from 2D layer to 1D band may occur for several reasons. First, F^- ions have the propensity, compared with O^{2-} ions that often bridge different metal centers, to form terminal sites on $[Ge(O/OH)_{6-x}F_x]^{z-}$ polyhedra. Second, the electron-withdrawing/sigma donor character of the F^- ion stabilizes the Ge^{4+} ions. Third, another important reason for F^- ions to be the terminals stems from the high oxidation states of Ge(4+) and P(5+).

According to Pauling's second rule of electrostatic neutrality,[37] every coordinating anion (assuming to be identical) of a Ge^{4+} octahedron receives 4/6 electrostatic bond strength. For a P^{5+} ion in tetrahedral coordination, every O atom gets 1.25 electrostatic bond strength. In the KFeGePOF compound, Ge is six-coordinated by four O atoms, one OH group, and one F

DOI: 10.1021/acs.inorgchem.5b00973
Inorg. Chem. 2015, 54, 6978−6985

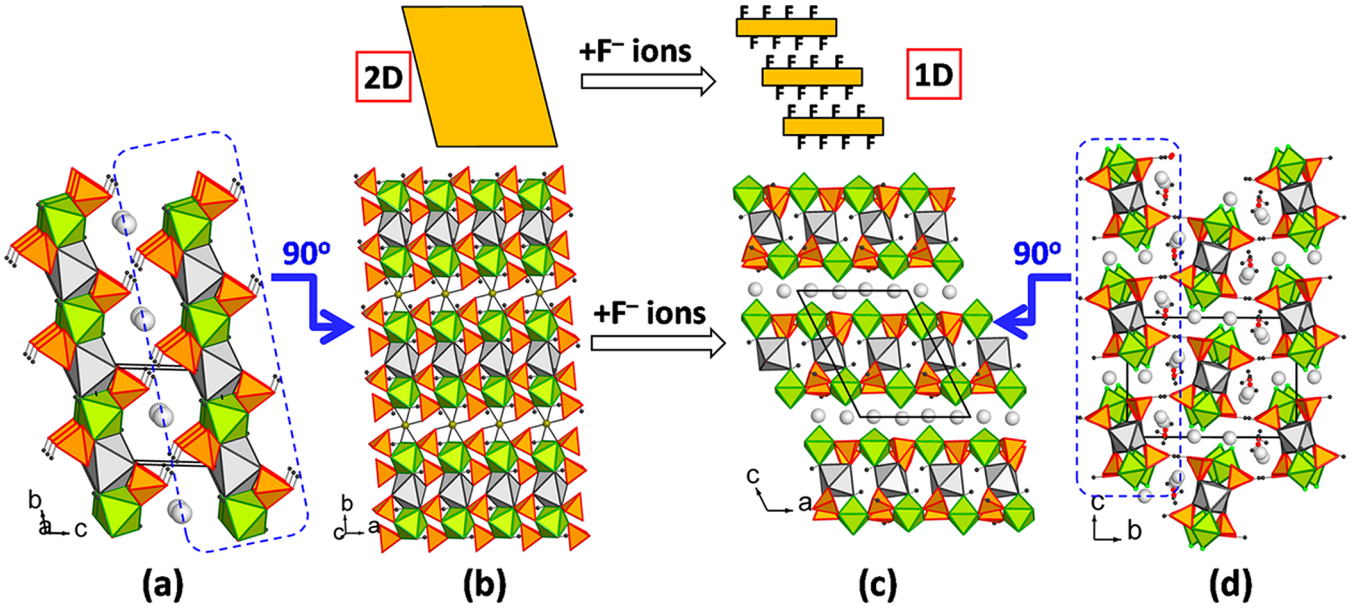

Figure 5. Schematic presentation shows the structural transformation from the 2D layered structure of KFeGePO-2 (a, b) to the 1D band structure of KFeGePOF (c, d) via the addition of $KF{\cdot}2H_2O$. The blue outlines in (a) and (d) mark the parts of the two structures for comparison in (b) and (c), respectively. (b) One layer of KFeGePO-2. (c) Band structure of KFeGePOF derive from the 2D layer by replacing half of the Fe atoms with K and one of the two OH groups with F. FeO_6 octahedra: light gray, $GeO_4(OH/F)_2$ octahedra: green, PO_4 tetrahedra: orange, Fe atoms: brown spheres, K atoms: light gray spheres, F atoms: green spheres, O atoms: red spheres, H atoms: dark gray spheres.

atom. The four equatorial O atoms bridge to P atoms, while the unique OH group links to an Fe atom. The electrostatic bond strength contribution from the four O atoms and one OH group is only 20/6 valence units, requiring the remaining F^- ion to be not connected with any other cations (i.e., a terminal position, 4/6 valence unit).

A similar tailor effect of fluoride has been observed in the tetravalence metal phosphates, that is, titanium phosphate[38,39] and zirconium phosphate system.[34,40] Vivani and coauthors have reported a dimensional reduction from layer to ribbon and even to chain in zirconium phosphates by increasing the F^- ion numbers in the coordination sphere of Zr.[34] Similar cases have also been found in the fluorinated titanium phosphates, for example, $(NH_4)_{0.16}K_{1.84}[Ti_2F_2(PO_4)_2(PO_3OH)]$[39] with a unique lamella framework and $K_{16}[Ti_{10}P_4O_{16}F_{44}]$[38] with cluster structure, where the F^- ions often acted as terminals. However, F^- ions can also act as bridging ligands that have been observed in the transition metal phosphates with low valence state, that is, Fe^{2+} and Co^{2+} fluorophosphates.[41] Therefore, whether to act as terminal or as bridge ligand of F^- ions is mainly influenced by the valence state and coordination number of the central metal atoms. For the high-valence metal phosphates, such as Ti^{4+}, Zr^{4+}, and Ge^{4+} phosphates, F^- ions prefer to be terminals but as bridge ligands in the divalent metal phosphates. Therefore, the tailor effect of fluoride forces the 2D layered structure of KFeGePO-2 to reduce to the 1D band structure of KFeGePOF in the GePOs system. This fluoride technique offers an attractive route to rationally design low-dimensional structures in the GePOs system, even to other tetravalent metal phosphates.

3.3. Infrared Spectroscopy. The FT-IR spectra of KMGePO-2 (M = Fe, Co) and KMGePOF (M = Fe, Co), shown in Figure 6, were recorded from powder samples mixed with KBr in a pressed pellet. Similar absorption bands observed in the spectra of the isotypic compounds further confirm the single-crystal analysis results. The detailed band data of the

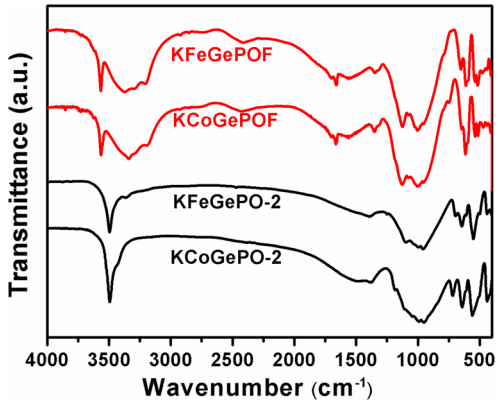

Figure 6. IR spectra of *KM*GePO-2 (*M* = Fe, CO; black) and *KM*GePOF (*M* = Fe, CO; red).

reported compounds are listed in the Supporting Information. In Figure 6, the two types of compounds have similar absorption bands in the low-frequency regions, which are mainly assigned to the vibrations of HPO_4, PO_4, and $GeO_4(OH)_2/GeO_4F(OH)$ groups. In the higher-frequency regions, however, the fluorinated derivative KFeGePOF has additional absorption bands at 3291 and 1660 cm^{-1}, which are attributable to the stretching vibration ($\nu_1(H_2O)$) and bending modes ($\delta_2(H_2O)$) of the molecular water.[42] In particular, the sharp and strong band at 3291 cm^{-1} indicates that the molecular water occupies a well-defined symmetry site. Therefore, FT-IR results confirm an additional water molecule in KFeGePOF, which is not observed in KFeGePO-2.

3.4. Thermal Properties. The TG curves (Figure 7 and Supporting Information, Figure S3) of the two KMGePO-2 compounds are similar and are both characterized by a single-step weight loss in the temperature range of 300−600 °C. Take the Fe compound as an example (Figure 7), the total weight loss of 6.99% fits well with the condensation of three OH

DOI: 10.1021/acs.inorgchem.5b00973
Inorg. Chem. 2015, 54, 6978−6985

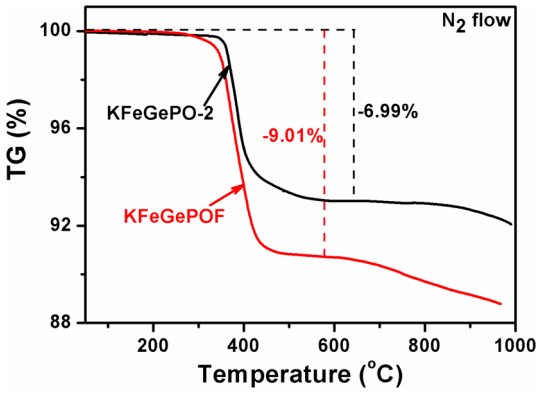

Figure 7. TG curves of *M*GePO-2 (*M* = Fe, Co) and *M*GePOF (*M* = Fe, Co).

groups per formula unit (Calc: 6.87%). For the fluorinated compounds, the TG curve of KFeGePOF has a two-step weight loss. The first step occurred in the temperature range from 150 to 500 °C and has a weight loss of 9.01%, which is in excellent agreement with the removal of two H_2O molecules and the condensation of four OH groups per formula unit (Calc: 8.76%). The second step with a continuous but slow weight loss above 500 °C is interpreted to represent the evaporation of F ions, which is commonly observed in both fluorogallophosphates and fluorinated zirconium phosphates.[43] For the fluorinated compounds, the extra water molecule in the formula may cause the earlier thermal decomposition.

Although dehydration of water molecules and condensation of hydroxyl groups often occur at different temperatures, it is not surprising to observe these two processes coalesce into a single step in KFeGePOF with extensive hydrogen bonding and strong K−Ow coordination. Here the Ow atom is fixed by three neighboring K atoms. It also interacts with the anionic bands via hydrogen bonds.

3.5. Magnetic Properties. Figure 8 shows that the temperature dependence of the magnetic susceptibility χ of

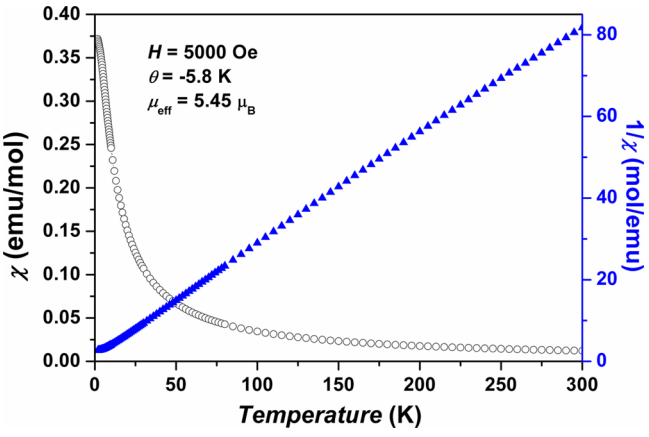

Figure 8. Temperature dependence of the molar magnetic susceptibility $\chi(T)$ and inverse molar magnetic susceptibility $\chi^{-1}(T)$ of KFeGePO-2 for an external field of 5000 Oe.

KFeGePO-2 obeys the Curie−Weiss law above 30 K at a magnetic field of H = 5000 Oe. An effective magnetic moment μ_{eff} per Fe atom was calculated to be 5.45 μ_B, which is consistent with Fe^{2+} in octahedral coordination. The small negative Weiss temperature (θ = −5.8 K) suggests that there is a weak antiferromagnetic long-range order of the Fe-moments at low temperatures. This suggestion is consistent with the Fe···Fe distances of 4.45 and 6.22 Å within the layer and 7.81 Å between the neighboring layers, which are probably too far for direct or strong Fe−Fe interactions.

4. CONCLUSION

A series of 2D layered $K[M^{II}Ge(OH)_2(H_{0.5}PO_4)_2]$ (*M* = Fe, Co) and another series of 1D band structure $K_4[M^{II}Ge_2F_2(OH)_2(PO_4)_2(HPO_4)_2]\cdot 2H_2O$ (M = Fe, Co) have been successfully synthesized by using an unconventional hydrothermal route and have been structurally characterized. The addition of $KF\cdot 2H_2O$ to the reaction mixture results in the structural dimensional reduction from a 2D layered structure to a 1D band structure, via the incorporation of F to the coordination sphere of germanium at a terminal position. Therefore, it may be concluded that whether to act as terminal or as bridge ligand of F^- ions is mainly influenced by the valence state and coordination number of the central metal atoms. For the high-valence metal phosphates, such as Ti^{4+}, Zr^{4+}, and Ge^{4+} phosphates, F^- ions prefer to be terminals but as bridge ligands in the divalent metal phosphates. This kind of top-down dimensional reduction strategy could be applied to synthesize new GePOs with low-dimensional structures by incorporating different amounts of fluorine into the frameworks. This strategy is opposite to the bottom-up structural assembly from phosphate to GePO via GeO_6 single chains, which was reported by our group recently.[25] These structural assembly and disassembly processes not only enrich the GePOs structure chemistry but also may be extended to other metal phosphate systems.

■ ASSOCIATED CONTENT

Ⓢ Supporting Information

Bond valence sum calculation results, SEM and EDX data, absorption bands of FT-IR spectra, magnetic susceptibility of KFeGePOF, and X-ray crystallographic information file (CIF) for all compounds, as well as TG curves of KCoGePO-2 and KCoGePOF. The Supporting Information is available free of charge on the ACS Publications website at DOI: 10.1021/acs.inorgchem.5b00973. Further crystallographic information (excluding structure factors) can be obtained free of charge from Fachinformationszentrum Karlsruhe, 76344, Eggenstein-Leopoldshafen, Germany (e-mail: crysdata@fiz-karlsruhe.de), on quoting the depository numbers CSD-429161, 429162, 429163, and 429164 for KFeGePO-2, KCoGePO-2, KFeGePOF, and KCoGePOF, respectively.

■ AUTHOR INFORMATION

Corresponding Author

*E-mail: yaxihuang@xmu.edu.cn. Phone: +86-13950175872. Fax: +86-592-2183937.

Author Contributions

The manuscript was written through contributions of all authors. All authors have given approval to the final version of the manuscript.

Notes

The authors declare no competing financial interest.

■ ACKNOWLEDGMENTS

This work was supported by the National Natural Science Foundation of China (Grant Nos. 21201144 and 21233004),

DOI: 10.1021/acs.inorgchem.5b00973
Inorg. Chem. 2015, 54, 6978−6985

the Fundamental Research Funds for the Central Universities (Grant No. 2013121020), and Natural Science and Engineering Research Council of Canada.

REFERENCES

(1) Mizushima, K.; Jones, P.; Wiseman, P.; Goodenough, J. *Mater. Res. Bull.* **1980**, *15*, 783−789.
(2) Walton, R. I.; Millange, F.; O'Hare, D.; Paulet, C.; Loiseau, T.; Ferey, G. *Chem. Mater.* **2000**, *12*, 1977−1984.
(3) Oliver, S.; Kuperman, A.; Ozin, G. A. *Angew. Chem., Int. Ed.* **1998**, *37*, 47−62.
(4) Wang, K.; Yu, J.; Song, Y.; Xu, R. *Dalton Trans.* **2003**, 99−103.
(5) Wang, H.; Yuan, H.; Sae Hong, S.; Li, Y.; Cui, Y. *Chem. Soc. Rev.* **2015**, *44*, 2664−2680.
(6) Greenfield, J. T.; Kamali, S.; Izquierdo, N.; Chen, M.; Kovnir, K. *Inorg. Chem.* **2014**, *53*, 3162−3169.
(7) Feng, S.; Xu, R. *Acc. Chem. Res.* **2001**, *34*, 239−247.
(8) Lin, Z.-E.; Yang, G.-Y. *Eur. J. Inorg. Chem.* **2010**, 2895−2902.
(9) Férey, G. *J. Fluorine Chem.* **1995**, *72*, 187−193.
(10) Natarajan, S.; Mandal, S. *Angew. Chem., Int. Ed.* **2008**, *47*, 4798−4828.
(11) Corma, A. *Chem. Rev.* **1997**, *97*, 2373−2420.
(12) Melot, B. C.; Tarascon, J.-M. *Acc. Chem. Res.* **2013**, *46*, 1226−1238.
(13) Whittingham, M. S.; Song, Y. N.; Lutta, S.; Zavalij, P. Y.; Chernova, N. A. *J. Mater. Chem.* **2005**, *15*, 3362−3379.
(14) Mayer, H.; Völlenkle, H. *Z. Kristallogr.* **1972**, *136*, 387−401.
(15) Alami, M.; Brochu, R.; Soubeyroux, J.; Gravereau, P.; Le Flem, G.; Hagenmuller, P. *J. Solid State Chem.* **1991**, *90*, 185−193.
(16) Brochu, R.; Loueer, M.; Alami, M.; Alquraoui, M.; Loueer, D. *Mater. Res. Bull.* **1997**, *32*, 113−122.
(17) Winand, J.; Rulmont, A.; Tarte, P. *J. Solid State Chem.* **1993**, *107*, 356−361.
(18) Zhao, D.; Xie, Z.; Hu, J.-M.; Zhang, H.; Zhang, W.-l.; Yang, S.-L.; Cheng, W.-D. *J. Mol. Struct.* **2009**, *922*, 127−134.
(19) Popa, K.; Wallez, G.; Bregiroux, D.; Loiseau, P. *J. Solid State Chem.* **2011**, *184*, 2629−2634.
(20) Engel, G.; Fischer, U. *Z. Kristallogr.* **1985**, *173*, 101−112.
(21) Li, J. M.; Ke, Y. X.; Zhang, Y. G.; He, G. F.; Jiang, Z.; Nishiura, M.; Imamoto, T. *J. Am. Chem. Soc.* **2000**, *122*, 6110−6111.
(22) Liu, Y.; Yang, X.-L.; Wang, G.-L.; Zhang, J.; Li, Y.-Z.; Du, H.-B.; You, X.-Z. *J. Solid State Chem.* **2008**, *181*, 2542−2546.
(23) Liu, Y.; Yang, X.-L.; Zhang, J.; Li, Y.-Z.; Song, Y.; Du, H.-B.; You, X.-Z. *Chem. Commun.* **2008**, 3145−3147.
(24) Huang, Y.-X.; Zhang, X.; Huang, X.; Schnelle, W.; Lin, J.; Mi, J.-X.; Tang, M.-B.; Zhao, J.-T. *Inorg. Chem.* **2012**, *51*, 3316−3323.
(25) Huang, Y.-X.; Liu, B.; Wen, L.; Zhang, X.; Sun, W.; Lin, J.; Huang, C.-Z.; Zhuang, R.-C.; Mi, J.-X.; Zhao, J.-T. *Inorg. Chem.* **2013**, *52*, 9169−9171.
(26) Norberg, S. T.; Gustafsson, J.; Mellander, B. E. *Acta Crystallogr., Sect. B: Struct. Sci.* **2003**, *59*, 588−595.
(27) Romano, R.; Ruiz, A. I.; Alves, O. L. *J. Solid State Chem.* **2004**, *177*, 1520−1528.
(28) Peters, L.; Evans, J. S. O. *J. Solid State Chem.* **2007**, *180*, 2363−2370.
(29) Wang, W.; Li, Y.; Liu, L.; Dong, J. X. *Dalton Trans.* **2012**, *41*, 10511−10513.
(30) Sheldrick, G. M. *Acta Crystallogr., Sect. A: Found. Crystallogr.* **2008**, *64*, 112−122.
(31) Mi, J. X.; Borrmann, H.; Zhang, H.; Huang, Y. X.; Schnelle, W.; Zhao, J. T.; Kniep, R. *Z. Anorg. Allg. Chem.* **2004**, *630*, 1632−1636.
(32) Brown, I. D.; Altermatt, D. *Acta Crystallogr., Sect. B: Struct. Sci.* **1985**, *41*, 244−247.
(33) Olshansky, J. H.; Blau, S. M.; Zeller, M.; Schrier, J.; Norquist, A. J. *Cryst. Growth Des.* **2011**, *11*, 3065−3071.
(34) Gatta, G. D.; Masci, S.; Vivani, R. *J. Mater. Chem.* **2003**, *13*, 1215−1222.
(35) Bircsak, Z.; Hall, A. K.; Harrison, W. T. A. *J. Solid State Chem.* **1999**, *142*, 168−173.
(36) Hawthorne, F. C.; Ferguson, R. B. *Acta Crystallogr., Sect. B: Struct. Sci.* **1975**, *31*, 1753−1755.
(37) Pauling, L. *The Nature of the Chemical Bond and the Structure of Molecules and Crystals: An Introduction to Modern Structural Chemistry*, 3rd ed.; Cornell University: Ithaca, NY, 1960; pp 543−562.
(38) Yang, S. H.; Li, G. B.; Blake, A. J.; Sun, J. L.; Xiong, M.; Liao, F. H.; Lin, J. H. *Inorg. Chem.* **2008**, *47*, 1414−1416.
(39) Yang, S. H.; Li, G. B.; Liu, W.; Wang, W.; Yan, Z. M.; Huang, Y. I.; Liao, F. H.; Lin, J. H. *Inorg. Chem.* **2009**, *48*, 5449−5453.
(40) Liu, L.; Li, J. P.; Dong, J. X.; Sisak, D.; Baerlocher, C.; McCusker, L. B. *Inorg. Chem.* **2009**, *48*, 8947−8954.
(41) Armstrong, J. A.; Williams, E. R.; Weller, M. T. *J. Am. Chem. Soc.* **2011**, *133*, 8252−8263.
(42) Nakamoto, K. *Infrared and Raman Spectra of Inorganic and Coordination Compounds*; Wiley Online Library: 1978.
(43) Dong, J. X.; Liu, L.; Li, J. P.; Li, Y.; Baerlocher, C.; McCusker, L. B. *Microporous Mesoporous Mater.* **2007**, *104*, 185−191.

DOI: 10.1021/acs.inorgchem.5b00973
Inorg. Chem. 2015, 54, 6978−6985